Stratospheric ozone intrusion events and their impacts on tropospheric ozone in the Southern Hemisphere

Jesse W. Greenslade[1], Simon P. Alexander[2,3], Robyn Schofield[4,5], Jenny A. Fisher[1,6], and Andrew K. Klekociuk[2,3]

[1]Centre for Atmospheric Chemistry, School of Chemistry, University of Wollongong
[2]Australian Antarctic Division, Hobart
[3]Antarctic Climate and Ecosystems Co-operative Research Centre, Hobart, Australia
[4]School of Earth Sciences, University of Melbourne
[5]ARC Centre of Excellence for Climate System Science, University of New South Wales
[6]School of Earth & Environmental Sciences, University of Wollongong

Correspondence to: Jesse Greenslade (jwg366@uowmail.edu.au)

Abstract. Stratosphere-to-troposphere transport (STT) provides an important natural source of ozone to the upper troposphere, but the characteristics of STT events in the southern hemisphere extratropics and their contribution to the regional tropospheric ozone budget remain poorly constrained. Here, we develop a quantitative method to identify STT events from ozonesonde profiles. Using this method we estimate the seasonality and quantify the ozone transported across the tropopause over Davis (69° S), Macquarie Island (54° S), and Melbourne (38° S). STT seasonality is determined by two distinct methods: a Fourier bandpass filter of the vertical ozone profile, and an analysis of the Brunt-Viäsälä frequency. Using a bandpass filter on 7–9 years of ozone profiles from each site provides clear detection of STT events, with maximum occurrences during summer and minimum during winter above all three sites. The majority of tropospheric ozone enhancements from STT events occur within 2.5 km, 3 km of the tropopause at Davis, and Macquarie Island. Events are more spread out at Melbourne, occurring frequently up to 7.5 km from the tropopause. The mean fraction of total tropospheric ozone attributed to STT during STT events is 2–4% at each site; however, during individual events over 10% of tropospheric ozone may be directly transported from the stratosphere. The cause of STTs is determined to be largely due to synoptic low pressure frontal systems, determined using coincident ERA-Interim reanalysis meteorological data. Ozone enhancements can also be caused by biomass burning plumes transported from Africa and South America, these are apparent during austral winter and spring, and are determined using satellite measurements of CO.

To provide regional context for the ozonesonde observations, we use the GEOS-Chem chemical transport model, which is too coarsely resolved to distinguish STT events but is able to accurately simulate the seasonal cycle of tropospheric ozone columns over the three southern hemisphere sites. Combining the ozonesonde-derived STT event characteristics with the simulated tropospheric ozone columns from GEOS-Chem, we conservatively estimate STT influx near the three sites and see TODO:

1 Introduction

Tropospheric ozone constitutes only 10% of the total ozone column but is an important oxidant and greenhouse gas which is toxic to life, harming natural ecosystems and reducing agricultural productivity. Over the industrial period, increasing tropospheric ozone has been estimated to exert a radiative forcing (RF) of 365 mWm^{-2} (Stevenson et al., 2013), equivalent to a quarter of the CO_2 forcing (?). While much tropospheric ozone is produced photochemically from anthropogenic and natural precursors, downward transport from the ozone-rich stratosphere provides an additional natural source of ozone that is particularly important in the upper troposphere (Jacobson and Hansson (2000) and references therein). The contribution of this source to overall tropospheric ozone budgets remains uncertain (Škerlak et al., 2014), especially in the southern hemisphere. While models show decreasing tropospheric ozone due to stratospheric ozone depletion propagated to the upper troposphere through vertical mixing (Stevenson et al., 2013), recent work based on the Southern Hemisphere ADditional OZonesonde (SHADOZ) network suggests increasing upper tropospheric ozone near southern Africa, most likely due to stratospheric mixing (?Thompson et al., 2014). Uncertainties in the various processes which produce tropospheric ozone limit predictions of future ozone-induced radiative forcing. Here we use a multi-year record of ozonesonde observations from sites in the southern hemisphere extratropics, combined with a global model, to better characterise the impact of stratospheric ozone on the tropospheric ozone budget in the southern hemisphere.

Stratosphere-to-troposphere transport (STT) primarily impacts the ozone budget in the upper troposphere but can also increase regional surface ozone levels above the legal thresholds set by air quality standards (???Langford et al., 2012; ?; Lin et al., 2015). In the western US, for example, deep STT events during spring can add 20-40 ppbv of ozone to the ground-level ozone concentration, which can provide over half the ozone needed to exceed the standard set by the U.S. Environmental Protection Agency (Lin et al., 2012, 2015). Another important region of STT is the Middle East, where surface ozone exceeds values of 80 ppbv in summer, with 10 ppbv from STT contribution (?). Estimates of the overall contribution of STT to tropospheric ozone vary widely (e.g., ????). Early work based on two photochemical models showed that 25-50% of the tropospheric ozone column can be attributed to STT events globally, with most contribution in the upper troposphere (?). In contrast, a more recent analysis of the Atmospheric Chemistry and Climate Model Inter-comparison Project (ACCMIP) simulations by Young et al. (2013) found STT is responsible for 540 ± 140 Tg yr^{-1}, equivalent to $\sim$11% of the tropospheric ozone column, with the remainder produced photochemically (Monks et al., 2015). This wide range in model estimates exists in part because STT is challenging to accurately represent, and better model resolution is necessary to simulate small scale turbulence. Observation-based process studies are therefore key in determining the relative frequency of STT events, with models then able to quantify STT impact over large regions. Ozonesondes are particularly valuable for this purpose as they provide multi-year datasets with high vertical resolution.

Lower stratospheric and upper tropospheric ozone concentrations are highly correlated (?), suggesting mixing across the tropopause mainly caused by the jet streams over the ocean. Extratropical STT events most commonly occur during synoptic-scale tropopause folds (???) and are characterised by tongues of high potential vorticity (PV) air descending to low altitudes. As these tongues become elongated, filaments disperse away from the tongue and mix irreversibly into the troposphere. STT

can also be induced by deep overshooting convection (**?**), tropical cyclones (**?**) and mid-latitude synoptic scale disturbances (e.g., **??**). STT events have been observed in tropopause folds around both the polar front jet (**??**) and the subtropical jet (**?**). A big influence on the high surface ozone concentrations over the eastern Mediterranean is stratospheric mixing and anticyclonic subsidence (Zanis et al., 2014). They are also observed near cut-off lows (**??**), so both regional weather patterns and stratospheric mixing are important to understand for STT analysis.

The strength (ozone enhancement above background levels), horizontal scale, vertical depth, and longevity of these intruding ozone tongues vary with weather, topography, and season. While the frequency, seasonality, and impacts of STT events have been well characterised in the tropics and northern hemisphere (NH), observational estimates from the southern hemisphere (SH) extra-tropics are noticeably absent in the literature. The role of STT in the SH remains highly uncertain due to the much more limited data availability compared to the NH and the temporal sparsity of these datasets (**?**Thompson et al., 2014; **?**).

Here, we characterise the seasonal cycle of STT events and quantify their contribution to the SH extratropical tropospheric ozone budget using nearly a decade of ozonesonde observations from three locations around the Southern Ocean spanning latitudes from 38°S-69°S. In Section 2 we describe the observations and the methods used to identify STT events and to relate STT occurrence to meteorological events. Section 3 provides our newly derived climatologies of STT frequency, seasonality, intrusion altitude, and depth, and Section 4 uses these new climatologies to evaluate upper tropospheric ozone in a global chemical transport model (GEOS-Chem). Finally, in Section 5 we use the observations and the model to estimate the overall contribution of STT events to total tropospheric ozone in the high southern latitudes.

2 Data and Methods

2.1 Ozonesonde record in the Southern Ocean

Ozonesondes provide a high vertical resolution profile of ozone, temperature, pressure, and humidity from the surface to 35 km. In the troposphere, the ozonesondes generally make 150-300 measurements. Ozone mixing ratio is quantified with an electrochemical concentration cell that senses the proportional electrical current from reaction of ozone with a solution of potassium iodide. Standardised procedures are followed when constructing, transporting, and releasing the ozonesondes http://www.ndsc.ncep.noaa.gov/organize/protocols/appendix5/. Ozonesondes are estimated to provide around 2% precision in the stratosphere, which improves at lower altitudes, and ozonesondes have been shown to be accurate to within 5% when the correct procedures are followed (**?**).

Ozonesondes are launched approximately weekly from Melbourne (38° S, 145° E), Macquarie Island (55° S, 159° E) and Davis (69° S, 78° E), as shown in Fig. 1. Melbourne, a major city in Victoria, Australia is in the far south eastern section of the Australian mainland, actual releases are north of the central business district in the Broadmeadows suburb. Macquarie island is isolated from the Australian mainland, situated in the remote southern ocean and unlikely to be affected by any local anthropogenic pollution events. Davis is on the coast of Antarctica and also unlikely to experience the effects of local pollution.

For this study, we use the 2004-2013 data for Melbourne and Macquarie and the 2006-2013 data for Davis because both ozone and geopotential height (GPH) profiles were measured during these periods. At Davis, ozonesondes are launched twice

Figure 1. Ozonesonde release sites and the regions which will be used to examine STT effect on tropospheric ozone levels.

Table 1. Number of sonde releases at each site over the period of analysis.

Site	Total Releases	Monthly Releases (J, F, M, ...)	Date Range
Davis	240	11, 12, 13, 12, 17, 31,	2006/04/13 -
		29, 28, 32, 28, 15, 12	2013/11/13
Macquarie	390	32, 31, 45, 28, 34, 33,	2004/01/20 -
		28, 35, 29, 33, 31, 31	2013/01/09
Melbourne	456	31, 38, 40, 38, 41, 36,	2004/01/08 -
		38, 39, 46, 40, 38, 31	2013/12/18

as frequently during the ozone hole season and preceding months (June-October) as at other times of year (**?**). A summary of ozonesondes at each site can be seen in Table 1.

Characterisation of STT events requires a clear definition of the tropopause. Two common tropopause height definitions are the standard lapse rate tropopause (**?**) and the ozone tropopause (**?**). The lapse rate tropopause is defined as the lowest altitude where the lapse rate (vertical gradient of temperature) is less than $2°C$ km^{-1}, provided the lapse rate between this altitude

5

4

and 2 km above is also below $2°C\ km^{-1}$. The ozone tropopause is defined as the lowest altitude satisfying the following three conditions for the ozone mixing ratio (OMR) (**?**):

1. Vertical gradient of OMR is greater than 60 ppb km^{-1};

2. OMR is greater than 80 ppb; and

3. OMR exceeds 110 ppb between 500 m and 2000 m above the altitude under inspection (modified to between 500 m and 1500 m in the Antarctic, including the site at Davis).

The ozone tropopause can be less robust during stratosphere-troposphere exchange; however, it is more robust than the lapse rate tropopause at polar latitudes in winter and near jet streams in the lower stratosphere due to temperature inversions near the tropopause (**???**). In this work, the lower of these two tropopause altitudes is used. We slightly alter the lapse rate tropopause definition so as only to detect tropopauses above 4 km altitude, since at all three sites we saw several false positive lapse-rate detections due to temperature inversions near 2 km in altitude. This choice avoids occasional unrealistically high tropopause heights due to perturbed ozone or temperature measurements in the ozonesonde data. Another commonly used tropopause definition (the dynamical tropopause) is determined from the ± 2 PVU isosurface, which allows a 3D view of folds and other tropopause features in a sufficiently resolved model (Škerlak et al., 2014).

Figure 2 shows the monthly median tropopause altitudes at each location (solid lines). At Melbourne, tropopause altitude displays a seasonal cycle with maximum in summer and minimum is winter. This seasonality is missing at Macquarie and almost reversed at Davis, which has a minimum during autumn and maximum from winter to spring. Tropopause altitude decreases with latitude from 9-12 km at Melbourne (38° S) to 7-9 km at Davis (69° S).

Figure 3 shows multi-year averaged ozone mixing ratios measured by ozonesonde over the three stations. Over Melbourne, increased ozone extending down through the troposphere is apparent from December to March and from September to November. The increased tropospheric ozone in these months is due to STT (in summer), and possible biomass burning influence (in spring), both discussed in more detail below. Over Davis and Macquarie Island, tropospheric ozone is higher between March and October, although the seasonal differences are small compared to those at Melbourne. This seasonality at the high latitude sites is driven by a decrease in photochemical destruction under the reduced radiation conditions around polar night.

2.2 Model description

To provide regional and global context to the ozonesonde observations, we use the GEOS-Chem version 10-01 global chemical transport model (**?**), which simulates ozone along with more than 100 other trace gases throughout the troposphere and stratosphere. Stratosphere-troposphere coupling is calculated using the stratospheric unified chemistry extension (UCX) (**?**). Transport is driven by assimilated meteorological fields from the Goddard Earth Observing System (GEOS-5) maintained by the Global Modeling and Assimilation Office (GMAO) at NASA. Ozone precursor emissions are from the Model of Emissions of Gases and Aerosols from Nature (MEGAN) version 2.1 (**?**) for biogenic emissions, the Emissions Database for Global Atmospheric Research (EDGAR) version 4.2 for anthropogenic emissions, and the Global Fire Emissions Database (GFED4) inventory (**?**) for biomass burning emissions. Our simulation was modified from the standard v10-01 to fix an error in the treatment
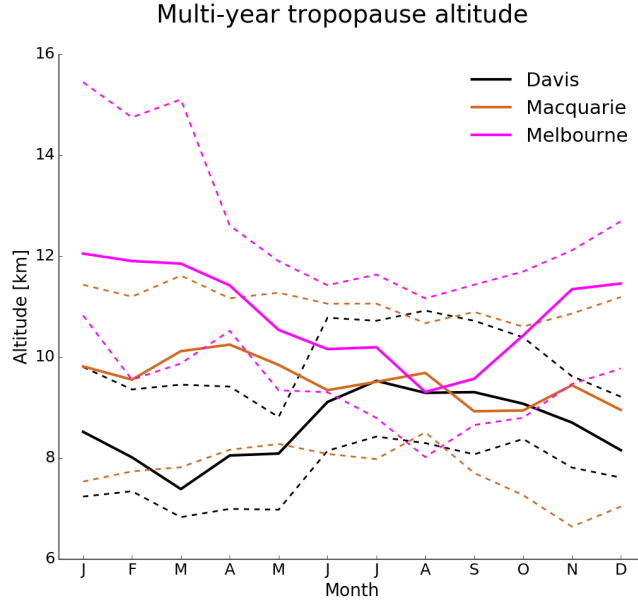
Figure 2. Multi-year monthly median tropopause altitude (minimum of lapse rate and ozone defined tropopause) determined from ozonesondes measurements at Melbourne (2004-2013), Macquarie (2004-2013) and Davis (2006-2013) (solid lines). Dashed lines show the 10th to the 90th percentile of tropopause altitude for each site.

of ozone data from the Total Ozone Mapping Spectrometer (TOMS) satellite used to calculate photolysis (see http://wiki.seas.harvard.edu/geos-chem/index.php/FAST-JX_v7.0_photolysis_mechanism#Fix_for_TOMS_to_address_strange_cycle_in_OH_output.).

Our simulations span 2005-2012 (following a 1-year spin-up) with horizontal resolution of $2°$ latitude by $2.5°$ longitude and 72 vertical levels from the surface to 0.01 hPa. The vertical resolution is finer near the surface at ~ 60 m between levels, spreading out to ~ 500 m near 10 km altitude, and reaching ~ 1500 m near the top of the atmosphere. For comparison to the ozonesonde observations, the model state was saved every 6 hours within the grid boxes containing each site. When comparing against ozonesondes, GEOS-Chem UTC+0 time samples are used for all sites. This means that the simulated ozone profiles are analysed at local times of 7AM for Davis, and 11AM for Macquarie and Melbourne. GEOS-Chem uses the tropopause height provided by GEOS-5 met fields which are calculated using a lapse-rate definition using the first minimum above the surface in the function $0.03 \times T(p) - log_{10}(p)$, with p in hPa and T being temperature as a function of pressure (**?**).

2.3 Characterisation of STT events and associated fluxes

We characterise STT events using the ozonesonde vertical profiles to identify tropospheric ozone enhancements above a local background (in moles per billion moles of dry air, referred to here as ppb). The process is illustrated in Figure 4 on an example ozone profile. First, the ozone vertical profiles are linearly interpolated to a regular grid with 20 m resolution from the surface
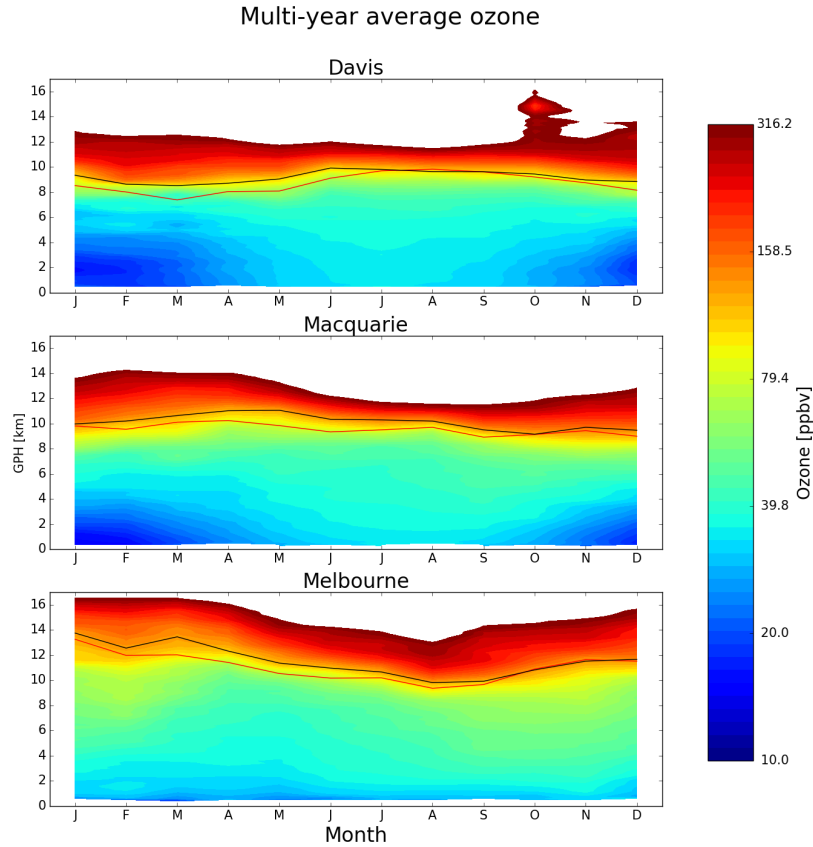
Multi-year average ozone

Figure 3. Multi-year mean seasonal cycle of ozone mixing ratio over Davis, Macquarie, and Melbourne as measured by ozonesondes. Measurements were interpolated to every 100 m and then binned monthly. Black and red solid lines show median ozone and lapse-rate defined tropopause altitudes (respectively), defined as described in the text.

to 14 km altitude. The interpolated profiles are then bandpass-filtered using a Fourier transform to retain perturbations with vertical scales between 0.5 km and 5 km (removing low and high frequency perturbations). In what follows, these filtered vertical profiles are referred to as perturbation profiles.

10   We assume that in the troposphere, the ozone profile is a simple summation of sine and cosine waves. Note that this would not really be the case if you include the stratosphere due to the sharp jump at the tropopause. Once the troposphere is split into wave sine and cosine wave functions we remove the waves with frequency outside of our chosen bandwidth (in this case the upper and lower frequency limits equate to our chosen vertical scale). This is done quickly using a fast fourier transform method (**?**), using IDL code written by Dr. Simon Alexander shown in a supplementary document (TODO:hardcode reference
15   here sup:sec:FFTCode).

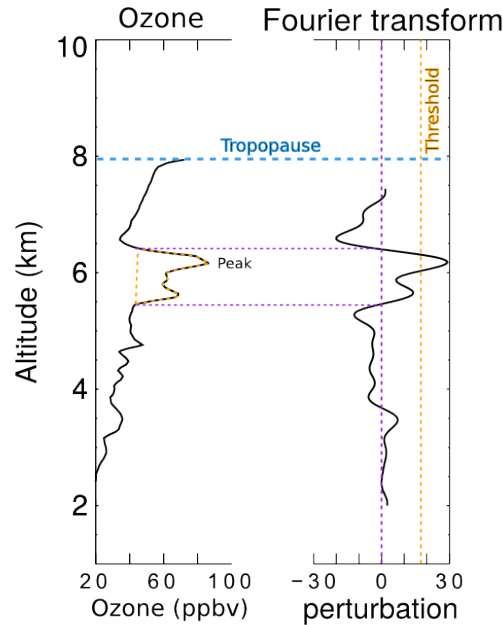## Ozone at Melbourne on 2004/01/08

Figure 4. An example of the STT identification and flux estimation methods used in this work. The left panel shows an ozone mixing ratio profile from Melbourne on 8 January 2004 from 2 km to the tropopause (blue dashed horizontal line). The right panel shows the perturbation profile created from bandpass filtering of the mixing ratio profile. The STT occurrence threshold calculated from the 99th percentile of all perturbation profiles is shown as the orange dashed line, and the vertical extent of the event is shown with the purple dashed lines (see details in text). The ozone flux associated with the STT event is calculated using the area outlined with the orange dashed line in the left panel.

The choice of band limits was set empirically in order to remove the slow positive gradient of ozone over altitude as well as any measurement noise. For an event to qualify as STT, a clear increase above the background ozone level is needed, as a bandpass filter leaves us with enhancements minus any noise or seasonal scale vertical profile effects. The 0.5 km scale limit is set in order to remove any spikes of ozone which could be considered noise. We next use all the perturbation profiles at each site to calculate the 99th percentile perturbation value for the site. The threshold is calculated from all the interpolated filtered values between 2 km above the surface and 1 km below the tropopause. This is our threshold for tropospheric ozone perturbations, and any profiles with perturbations exceeding this value in individual ozonesondes are classified as STT events. STT events at altitudes below 4 km are removed to avoid surface pollution, and events within 0.5 km of the tropopause are removed to avoid false positives induced by the sharp transition to stratospheric air.

We define the ozone peak as the altitude where the OMR is greatest within the lowest range of altitudes over which the perturbation profile exceeds the percentile-based threshold. The STT event is confirmed if the perturbation profile drops below zero between the ozone peak and the tropopause. Alternatively, the STT event is also confirmed if the OMR between the

ozone peak and the tropopause drops below 80 ppb and is at least 20 ppb lower than the OMR at the ozone peak. If neither of these conditions are met, the profile is rejected as a non-event. This final step removes near-tropopause anomalies for which there is insufficient evidence of detachment from the stratosphere. Vertical ozone profiles recorded by ozonesondes are highly dependent on the time of launch (**?**), and it cannot be guaranteed that detected ozone enhancements are fully separated from the stratosphere, although this method minimises that risk by removing detected events too near the tropopause.

We estimate the ozone flux into the troposphere associated with each event by integrating the ozone concentration enhancement vertically over the altitude range for which an STT event is identified (i.e. enhancement near the ozone peak over which the perturbation profile is greater than zero). This estimate is conservative because it does not take into account any ozone enhancements outside of the detected peak that may have been caused by the STT, and also ignores any enhanced ozone background amounts from synoptic-scale stratospheric mixing into the troposphere.

Our method differs somewhat from that used by **?** to detect STT events from ozonesonde measurements. Their definition is based on subjective analysis of sondes released from 20 stations ranging in latitude from 35° S to 40° N. They identify an STT event if, starting from 5 km altitude, ozone exceeds 80 ppb and then within 3 km decreases by 20 ppb or more to a value less than 120 ppb. Their technique would miss many events due to the lower ozone concentrations found in the cleaner Southern Hemisphere (SH).

2.4 Biomass burning influence

The STT detection algorithm described in Sect. 2.3 assumes all mid-upper troposphere ozone perturbations above the 99th percentile are caused by stratospheric intrusions. In some cases, however, these perturbations may in fact reflect ozone production in lofted smoke plumes. Biomass burning in southern Africa and South America has previously been shown to have a major influence on atmospheric composition in the vicinity of our measurement sites (**???**), particularly from July to December (Pak et al., 2003; **?**). On occasion, smoke plumes from Australian and Indonesian fires can also reach the mid-high southern latitudes, as seen from satellite measurements of carbon monoxide (CO) discussed below.

Large biomass burning events emit substantial quantities of ozone precursors, some of which are capable of being transported long distances and driving ozone production far from the fire source (Jaffe and Wigder, 2012). Ozone production from biomass burning is complex and affected by photochemistry, fuel nitrogen load, and time since emission, among other factors. While ozone production occurs in some biomass burning plumes, this is not always the case; therefore ozone perturbations detected during transported smoke events may or may not be caused by the plume. For this reason all detected STT events found near (within ∼150 km of) smoke plumes are flagged, following visual inspection. Calculations of seasonality, and ozone flux do not include flagged events, however they are included in summary plots in this work.

Possible biomass burning influence is identified using satellite observations of CO from the AIRS (Atmospheric Infra-red Sounder) instrument on board the Aqua satellite (**?**). CO is emitted during incomplete combustion and is an effective tracer of long-range transport due to its long lifetime (**??**). In the Southern Hemisphere, biomass burning is the primary source of CO, making CO a good proxy for fire plumes (e.g., **??**). To identify possible biomass burning influence, AIRS vertical column CO
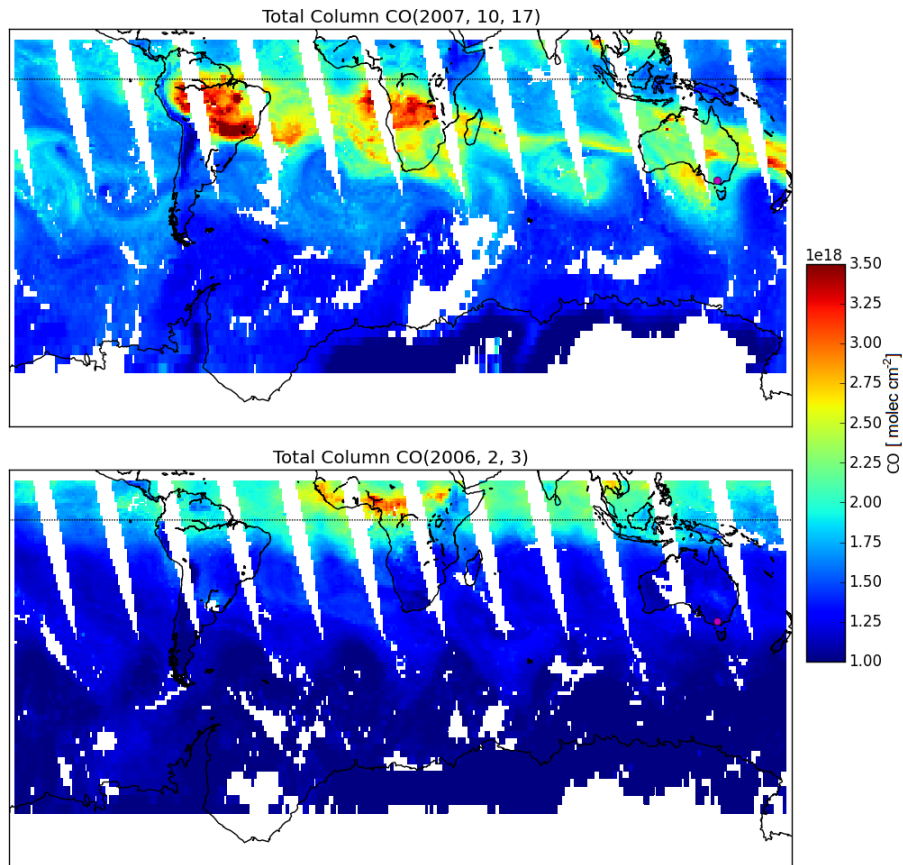
Figure 5. Example detection of biomass burning influence using AIRS total column CO. The top panel (17 October 2007) shows a day when ozone above Melbourne (purple dot) could have been caused by a transported biomass burning plume, and so was flagged in subsequent analysis. The bottom panel (3 February 2006) shows a day when Melbourne ozone was not influenced by transported smoke.

15 is visually inspected for all dates with detected STT events. Smoke plumes are diagnosed over areas with elevated CO columns ($\sim 2 \times 10^{18}$ molecules cm^{-2} or higher), and any sonde-detected STT event that occurs near a smoke plume is flagged.

Figure 5 contrasts two days; one with and one without signs of biomass burning influence near the Melbourne site (purple circle). On 17 October 2007 (top) elevated CO suggests the site may have been influenced by long-range transport from African and/or South American biomass burning. In contrast, on 3 February 2006 (bottom) CO columns across the SH show

20 no influence from biomass burning. All days with detected STT events were screened, with the exception of one event during which there were no available AIRS data (January 2010). We find that biomass burning may have influenced 14 events over Melbourne and 8 events over Macquarie island. These events are flagged in the following sections, and are not used in our calculation of total STT flux. All of the flagged events except for one (in January at Macquarie Island) occurred during the SH burning season (July to December, **?**). No events at Davis were seen to be influenced by smoke transport.

2.5 Classifying synoptic conditions during STT events

Data from the European Centre for Medium-range Weather Forecasts (ECMWF) Interim Reanalysis (ERA-I) (**?**) product are used for synoptic-scale examination of weather patterns over our three sites on dates matching detected STT events. We use the ERA-I 500 hPa data to subjectively classify the events based on their likely meteorological cause, examining each date where an event was detected. During STT occurrence, the upper troposphere is typically characterised by nearby low pressure fronts or cut-offs. Over Melbourne and Macquarie Island, we find that frontal and low pressure activity are prevalent during STT events (see Sect. 3). Over Davis, the weather systems are harder to distinguish. The stratospheric polar vortex may create ozone folds without other sources of upper tropospheric turbulence.

We examine two case studies in detail to illustrate the relationship between synoptic-scale conditions and STT events over Melbourne. Figure 6 (left) shows the ozone profile on 3 February 2005. The tropopause was between 400 and 500 hPa and ozone in the upper troposphere was anticorrelated with relative humidity, suggesting the ozone enhancements derived from dry stratospheric air. An ozone intrusion into the troposphere at $\sim$520 hPa was identified by our detection algorithm. The right panel shows the concurrent synoptic weather system, a cut-off low pressure system that caused a large storm and lowered the local tropopause height for several days. The flux of stratospheric ozone into the troposphere associated with this event, calculated using the method shown in Sect. 2.3, was at least 3.1×10^{11} molecules cm^{-3}, or 8% of the tropospheric ozone column.

Figure 7 (left) shows the ozone profile over Melbourne on 13 January 2010. The tropopause was higher on this date (120-160 hPa). Using our algorithm, we detected an ozone intrusion centred around 200 hPa. As before, ozone anti-correlation with relative humidity provides further evidence that the elevated ozone was stratospheric in origin. In this profile, there was clear separation between the detected intrusion (highlighted in pink) and the ozone tropopause (black dashed line), which indicates that the sonde passed through regular tropospheric air after hitting a stratospheric intrusion but before reaching the tropopause. The right panel shows that this event was associated with a trough (front) of low pressure passing over south eastern Australia. This front travelled from west to east and caused a wave of lowered tropopause height. Frontal passage is a known cause of STT as stratospheric air descends and streamers of ozone-rich air break off and mix into the troposphere (**?**).

3 STT event climatologies

Figure 8 shows the seasonal cycles of STT frequency at Davis, Macquarie Island, and Melbourne. Frequency is determined as detected event count divided by total launched ozonesondes for each month. STT events in Figures 8-11 are coloured based on the meteorological classification described in Sect. 2.5, with events classified as either low pressure fronts ("frontal", dark blue), cut-off low pressure systems ("cutoff", teal), or indeterminate ("misc", cyan). Events that may have been influenced by transported smoke plumes (Sect. 2.4) are shown in red. Ozonesonde releases are summarised in Table 1 and detected event counts are summarised in Table 2.

There is an annual cycle in the frequency of STT events (Fig. 8) with a summertime peak at all three sites. This summertime peak is due to a prevalence of summer low-pressure storms and fronts, which increase turbulence and lower the tropopause
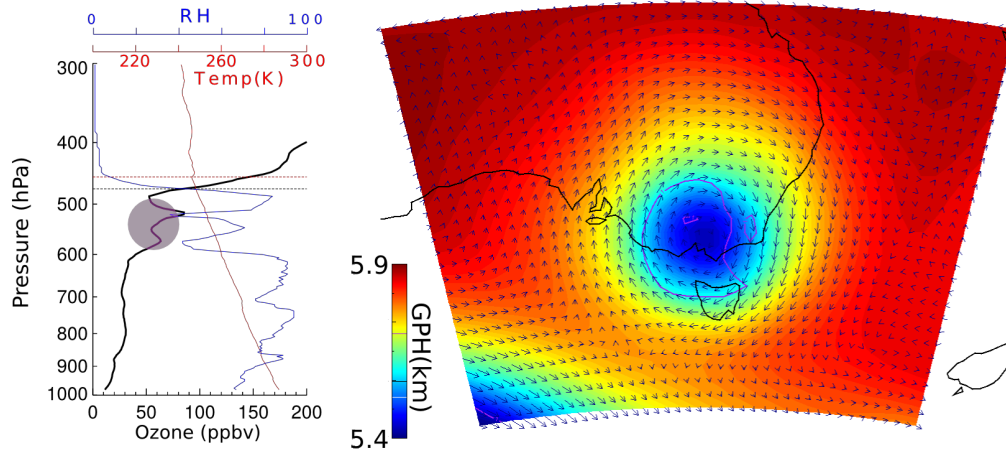
Figure 6. (Left) Vertical profile of ozone (black), relative humidity (blue), and temperature (red) measured by ozonesonde over Melbourne on 3 February 2005. The detected ozone STT event is highlighted in pink. Tropopause heights using both the ozone definition (black dashed line) and lapse rate definition (red dashed line) are also shown. (Right) Geopotential heights at 500 hPa from the ERA-Interim reanalysis, with wind vectors over-plotted. Also shown is the 1 PVU contour line (purple).

Table 2. Total number of ozonesonde detected STT events, along with the number of events in each category (see text).

Site	Events	Cut-offs	Frontals	Misc	Fire
Davis	46	7	20	19	0
Macquarie	47	10	20	9	8
Melbourne	73	12	34	13	14

(Reutter et al., 2015). At Davis, there is increased Antarctic winter activity, which may be due to the polar vortex and it's associated lowered tropopause and increased turbulence. STT events associated with cut-off low pressure systems are more prevalent during summer (winter for Davis), while STT events associated with frontal passage occur throughout the year.

This seasonality is not seen in the recent ERA-Interim tropopause fold analysis performed by **?**, where a winter maximum of ozone fold frequency ($\sim 0.5\%$ more folds in winter) over Australia can be seen. However their winter maximum is in the subtropics only - from around $20°$ S to $40°$ S, which can be seen as the prevalent feature over Australia in Fig. 5 of their publication. Wauben et al. (1998) look at modelled (CTM driven by ECMWF output) and measured ozone distributions and find more SH ozone in the lower troposphere during Austral winter, however they note that the ECMWF fields are uncertain here again due to lack of measurements. Their work shows a generally cleaner lower troposphere in the SH summer but can
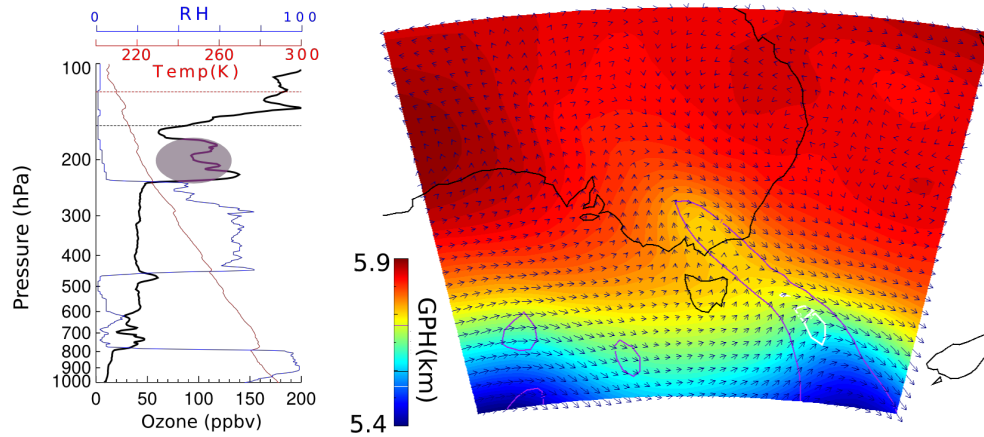
Figure 7. Same as Fig. 6 but for 13 January 2010. Also shown in this figure is the 2 PVU contour (white), often used to determine dynamical tropopause height.

not be construed to suggest more or less STT folds in either season. **?** examine modelled STT folds using ECMWF output over March 2000 - April 2001, and show that for this year there is a clear Austral winter maximum, again over the $20°$ S to $40°$ S band. The winter maximum does not include Melbourne, or the southern ocean, which may help explain why we see a seasonality which disagrees with these prior studies.

The measurement sites are not in the regions which have a clear winter maximum seen in Fig. 1 of **?**, and the large scale winter maximum shown by all three studies seems to be dominated by the system in that region. The seasonality of our three sites is not driven by the larger STT system seen over the southern Indian ocean and middle Australia which dominates prior analysis near or over Australia.

To examine the robustness of the distributions shown in Fig. 8, we developed an alternative assessment of the seasonal occurrence of STT events, with results shown in Fig. 9. Here STT occurrence is evaluated by consideration of the square of the dry Brunt-Viäsälä frequency (N^2) at the heights of the ozone tropopause (z_{OT}) and lapse rate tropopause (z_{LRT}) in each ozonesonde profile that has been binned to 500 m resolution. We use N^2 to assess atmospheric stability, which is normally distinctly higher in the stratosphere than in the troposphere, and assume that the vertical temperature gradients within the intrusion respond most rapidly to transported heat, which is an additional characteristic of stratospheric air. The altitude binning chosen is a compromise between vertical resolution and the level of variability in N^2 introduced by temperature gradients associated with perturbations from gravity waves and changes near the lapse rate tropopause, and is the minimum that produces a robust seasonal distribution. We define STT as having taken place if $N^2(z_{OT}) > N^2(z_{LRT})$ and $z_{OT} < z_{LRT}$; in this way the characteristically higher static stability and ozone concentration of stratospheric intrusion is regarded as being retained as it
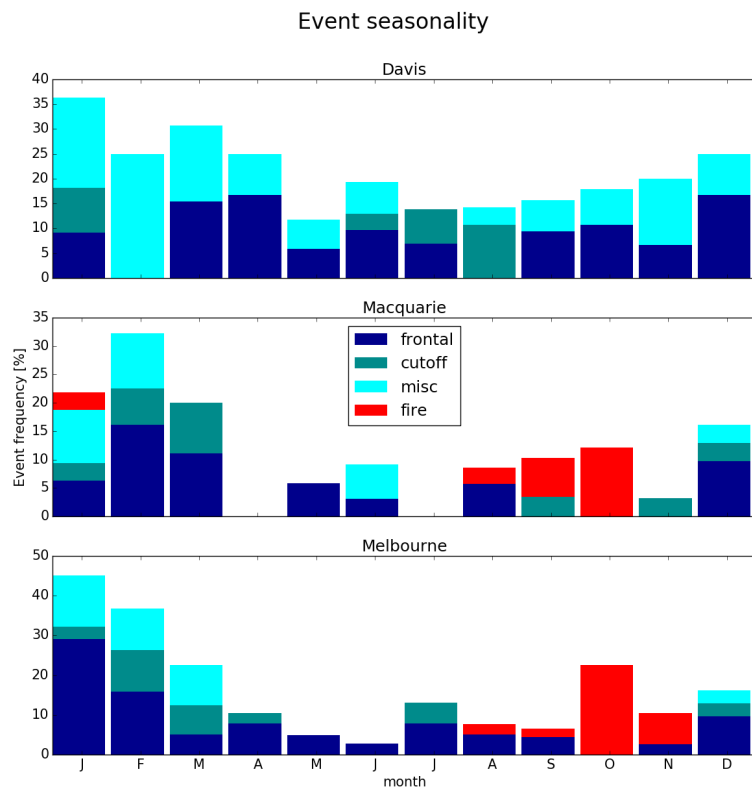
Figure 8. Seasonal cycle of STT event frequency at Davis (top), Macquarie Island (middle), and Melbourne (bottom). Events are categorised by associated meteorological conditions as described in the text, with low pressure fronts ("frontal") in dark blue, cut-off low pressure systems ("cutoff") in teal, and indeterminate meteorology ("misc") in cyan. Events that may have been influenced by transported smoke plumes are shown in red (see text for details).

penetrates below the lapse rate tropopause. The seasonal distributions shown for the three stations in Fig. 9 are generally similar to those shown in Fig. 8 (although detected events are less frequent), with the main exception that no events are identified with the alternative method at Davis in the first half of the year. From December to June, ozonesondes are generally only launched monthly at Davis, and the lack of STT events in these months for Davis potentially reflects the fewer measurement opportunities.

Figure 10 shows the altitudes of detected events, based on the altitude of peak tropospheric ozone (local maximum ozone within enhancement altitude) in the ozonesonde profile. STT event peaks most commonly occur at 6–10 km above Melbourne and 6–9 km at Davis but are distributed more evenly at Macquarie Island from 4–7.5 km. There is no clear relationship between meteorological conditions and event altitude.
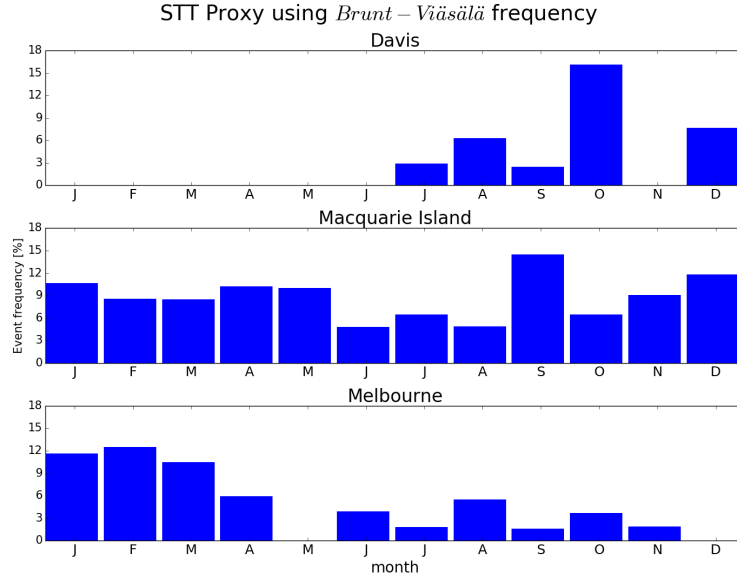
Figure 9. Seasonal distribution of STT events using the alternative STT proxy, obtained from consideration of the static stability at the ozone and lapse rate tropopauses, for Davis (2003-2012), Macquarie Island (1994-2012) and Melbourne (1999-2012).

Figure 11 shows the distance from the event peak to the tropopause (using the lowest of the two tropopause definitions), referred to as event depth. The majority of STT events occur within 3 km of the tropopause at Macquarie Island, and within 2.5 km of the tropopause at Davis. Over Melbourne, the event depth is more spread out, and peak ozone enhancement generally occurs within 6 km of the tropopause. Again, there is no clear relationships between meteorological conditions and event depth.

4 Simulation of southern regions of ozone columns

Figure 12 compares the time series of tropospheric ozone columns (Ω_{O_3}) in molecules cm^{-2} simulated by GEOS-Chem (red) to the measured tropospheric ozone columns (black). Observed tropospheric columns are calculated from the ozonesondes by calculating the ozone number density (molec cm^{-3}) using measured ozone partial pressure (P$_{O_3}$) and integrating over the measured GPH up to the tropopause:

$$\Omega_{O_3} = \int_0^{TP} \frac{P_{O_3}(z)}{k_B \times T(z)} \mathrm{d}z \tag{1}$$

where z is the altitude (GPH), TP is the altitude at the tropopause, T is the temperature, and k_B is the Boltzmann constant. GEOS-Chem outputs ozone density (molecules cm^{-3}), and height of each simulated box, as well as which level contains the tropopause, allowing modelled Ω_{O_3} to be calculated as the product of density and height summed up to the box below the
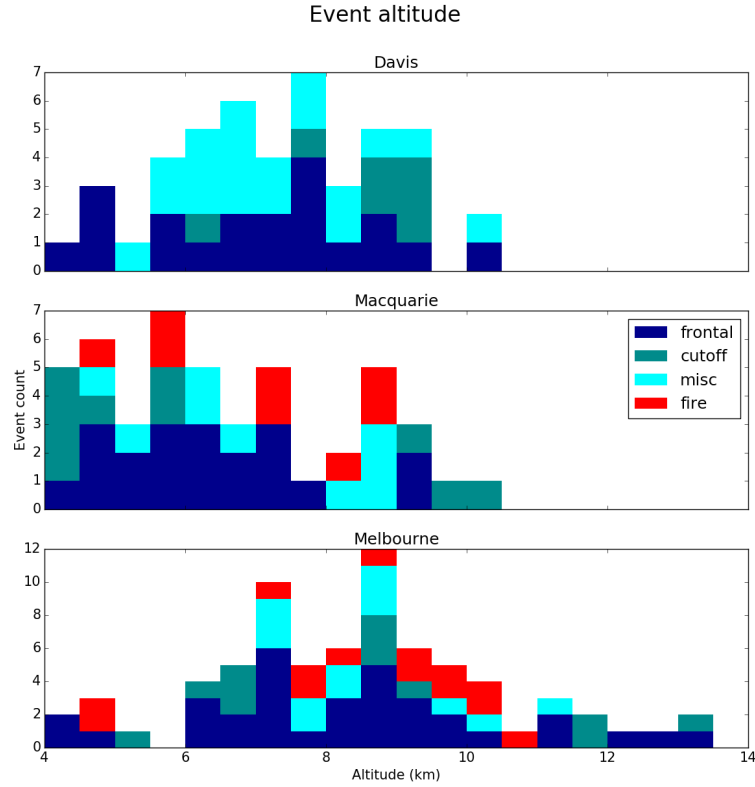
15

Figure 10. The distribution of STT event altitude at Davis (top), Macquarie Island (middle), and Melbourne (bottom), determined as described in the text. Events are coloured as described in Fig. 8.

tropopause level. In both observations and model, the maximum ozone column at Melbourne occurs in austral summer, with a
5 minimum in winter, while Macquarie and Davis show the opposite seasonality.

GEOS-Chem provides a reasonable simulation of the observed seasonality and magnitude of Ω_{O_3}. Reduced major axis regression of observed versus simulated Ω_{O_3} gives a line of best fit with slopes of 1.08 for Davis, 0.99 for Macquarie, and 1.34 for Melbourne. The model is only partially able to reproduce the variability in the observations, with paired r^2 values for of 0.38 for Davis, 0.18 for Macquarie, and 0.37 for Melbourne. Much of the variability is driven by the seasonal cycle, and after removing this effect (by subtracting the multi-year monthly means), the r^2 values decrease to .07, .11, .30 respectively, although the slope improves at Melbourne to 1.08.

Figure 13 shows the observed and simulated ozone profiles at all sites, averaged seasonally. The model generally underestimates ozone in the lower troposphere (up to 6 km) at both Davis and Macquarie, although this bias is less pronounced
5 during summer. Over Melbourne, ozone in the lower troposphere is well represented, but the model overestimates ozone from around 4 km to the tropopause. Similarly over Macquarie we see model overestimation of ozone above 4 km, suggesting that
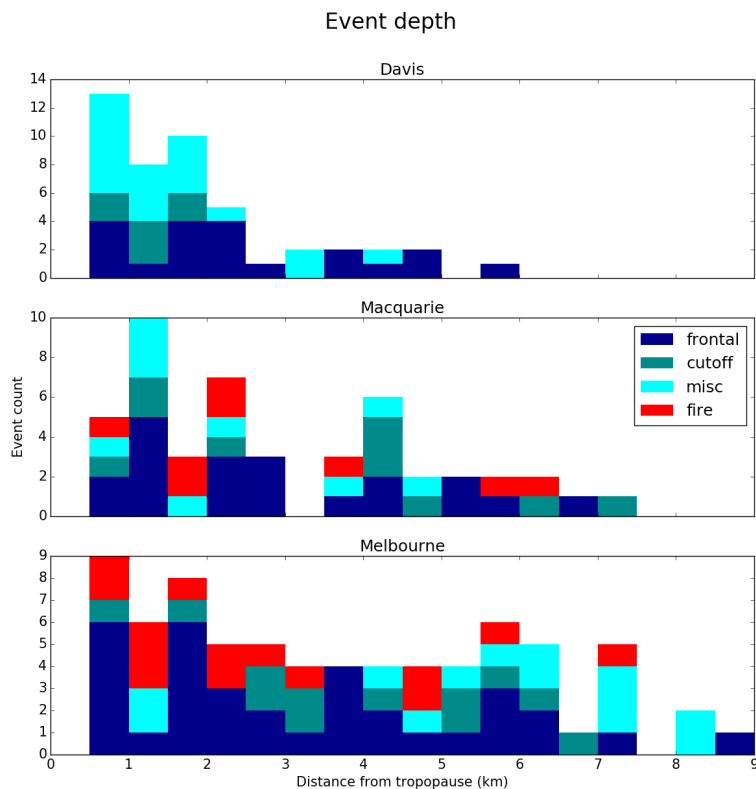
Event depth

Figure 11. The distribution of STT event depth, defined as the distance from the event to the tropopause, at Davis (top), Macquarie Island (middle), and Melbourne (bottom), determined as described in the text. Events are coloured as described in Fig. 8.

Macquarie may be influenced by processes seen at both of our other sites. Also shown is the tropopause height simulated by the model (horizontal dashed red line), the mean of which is always higher than the observed average, although this difference is not statistically significant. The effect of local pollution over Melbourne during austral summer (DJF) can be seen from the increased mean mixing ratios and enhanced variance near the surface. The gradient of the O$_3$ profiles is steeper in the measurements than the model, at all sites during all seasons.

GEOS-Chem does not have the vertical resolution required to capture STT events. Figure 14 compares modeled (red) and observed (black) ozone profiles on three example days when STT events were detected using the ozonesondes. The figures show the profile for each site with the closest (qualitative) match between model and observations. The vertical resolution of GEOS-Chem in the upper troposphere is too low to consistently allow detection of STTs, although in a few cases (e.g., Melbourne in Fig. 14) it appears that the event was large enough to be visible in the model output.
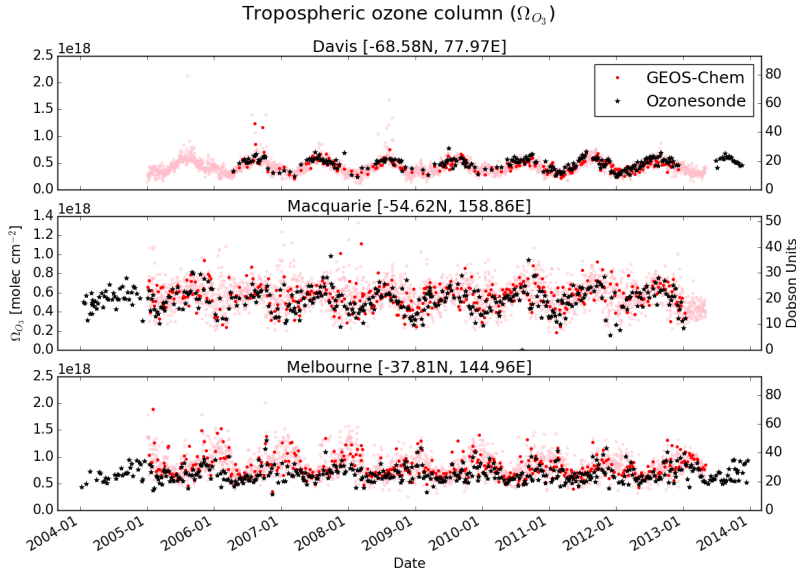
Figure 12. Comparison between observed (black) and simulated (pink, red) tropospheric ozone columns (Ω_{O3}, in molecules cm^{-2}) from 1 January 2004 to 30 April 2013. For the model, daily output is shown in pink, while output from days with ozonesonde measurements are shown in red. For each site, the model has been sampled in the relevant grid square.

5 Stratosphere-to-troposphere ozone flux from STT events

5.1 Method

We quantify the mean stratosphere-to-troposphere ozone flux due to STT events at each site based on the integrated ozone amount associated with each STT event (see Sect. 2.3). Events that may have been influenced by transported biomass burning are excluded from this calculation. Our estimate provides a preliminary estimate of how much ozone is transported from the stratosphere by the events detected by our method. The estimate is conservative for several reasons: it ignores secondary ozone peaks which may also be transported from the stratosphere, it ignores potential ozone enhancements which may have dispersed and increased the local background mixing ratio, and any influence from STT events advected into our measuremente region,
5   which may have increases the local background ozone.

Figure 15 shows the mean fraction of total tropospheric column ozone (calculated from ozonesonde profiles) attributed to stratospheric ozone intrusions at each site, averaged over days when an STT event occurred. At all sites, the mean fraction of tropospheric ozone attributed to STT events is 2–4%. On individual days at Macquarie and Melbourne, this value can exceed 10%. Figure 16 shows the STT-induced ozone flux in absolute terms. We find that the mean ozone flux associated with STT
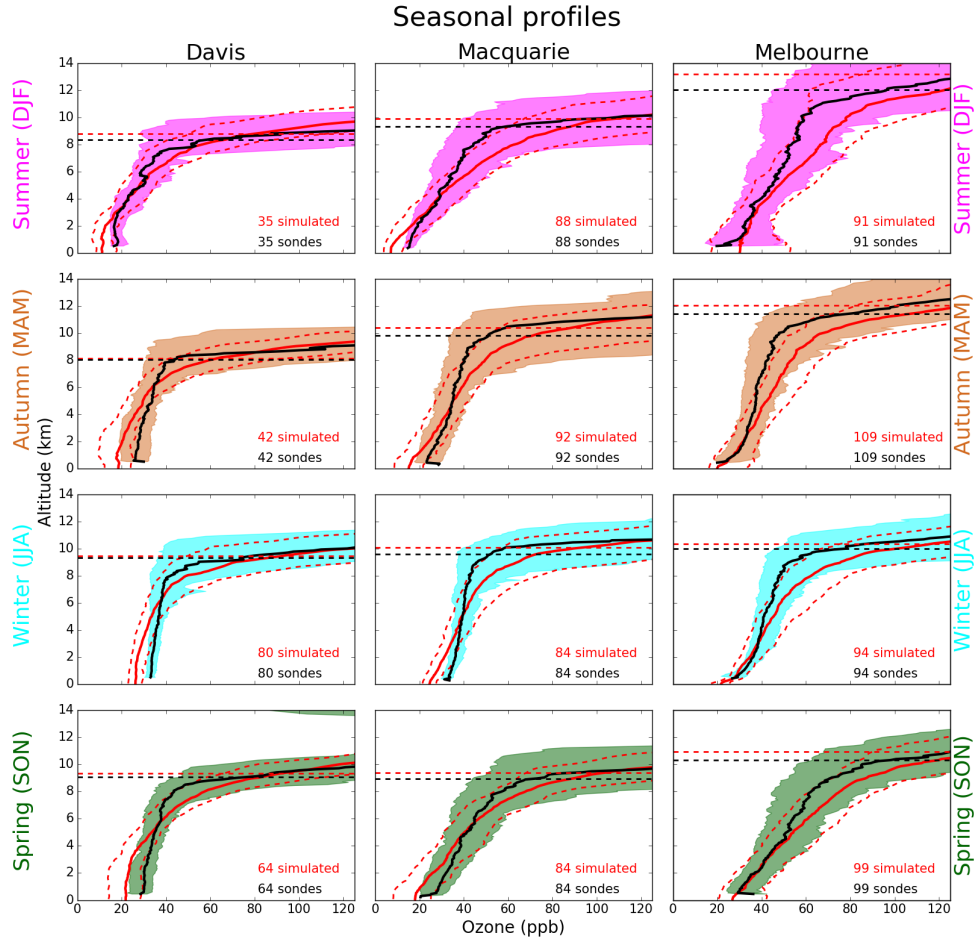
18

Figure 13. Observed and simulated tropospheric ozone profiles over Davis, Macquarie, and Melbourne, averaged seasonally. Model means (2005-2013 average) are shown as red solid lines, with red dashed lines showing the 10th and 90th percentiles. Ozonesonde means (over each season, for all years) are shown as black solid lines, with coloured shaded areas showing the 10th and 90th percentiles. The horizontal dashed lines show the mean tropopause heights from the model (red) and the observations (black).
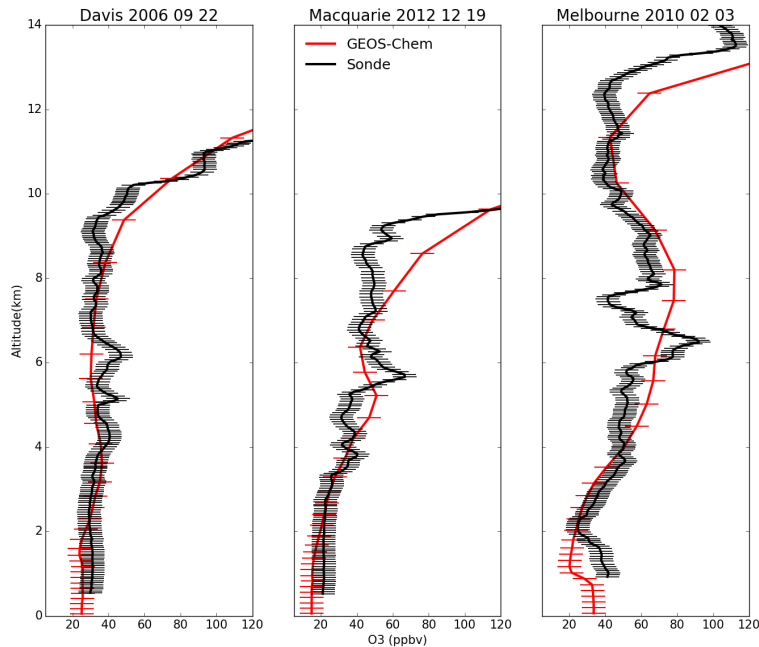
Figure 14. Example comparisons of ozone profiles from ozonesondes (black) and GEOS-Chem (red) from three different dates during which STT events were detected from the measurements. The dates were picked based on subjective visual analysis. The examples show the best match between model and observations for each site. GEOS-Chem pressure levels are marked with a dash.

events is $1\text{-}2 \times 10^{16}$ molecules cm^{-2}. Our flux estimates are relatively insensitive to our biomass burning filter: including smoke-influenced days changed the mean flux by less than 5% relative to the absolute values.

5   Three regions are used to examine possible STT flux over a larger area using modeled tropospheric ozone concentrations. The regions are shown in Fig. 1. The regions are centred at each site, and cover the site plus or minus ten degrees latitude, plus or minus 25, 16, and 11 degrees longitude for Davis, Macquarie Island, and Melbourne respectively. These boundaries provide a square (approximately) centred around each site with ~ 2000 km side lengths. The regions thus describe $\sim TODO : X$ million square km, for Davis, Macquarie Island, and Melbourne respectively. Davis has an estimated STT ozone contribution

10   of TODO:$\sim X \times 10^{17}$ molecules cm^{-2} a^{-1} or equivalently TODO:X Tg a^{-1}. TODO: also numbers for Mac/Melb.

    To determine the ozone column attributable to STT, we determine monthly averaged STT impact (I; fraction of tropospheric ozone sourced from the stratosphere) and the monthly mean tropospheric ozone column (from the GEOS-Chem multi-year mean, $\Omega_{Trop_{O_3}}$) over the regions described above. This can be expressed simply as the STT flux per event (flux$_i$ in each month: flux$_i = \Omega_{SO_{O_3}} \times I$. Next we determine how many events are occuring per month by assuming only one event can occur at one time, and that no event is measured twice. These assumptions allow a simple estimate of events per month from the relatively sparse dataset, and as long as our regions of extrapolation aren't too large, should be true. The monthly (P)robability
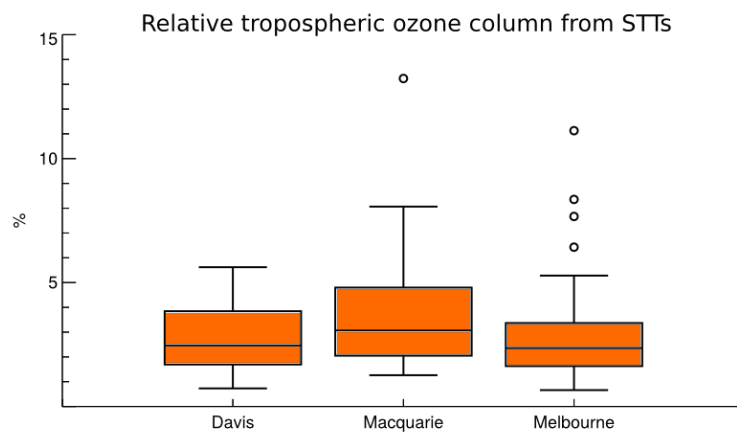
Figure 15. Percent of total tropospheric column ozone attributed to STT events, derived from ozonesonde measurements as described in the text. Box shows the interquartile range (IQR), with the centre line being the median, whiskers show the minimum and maximum, circles show values which lie more than 1.5 IQR from the median.
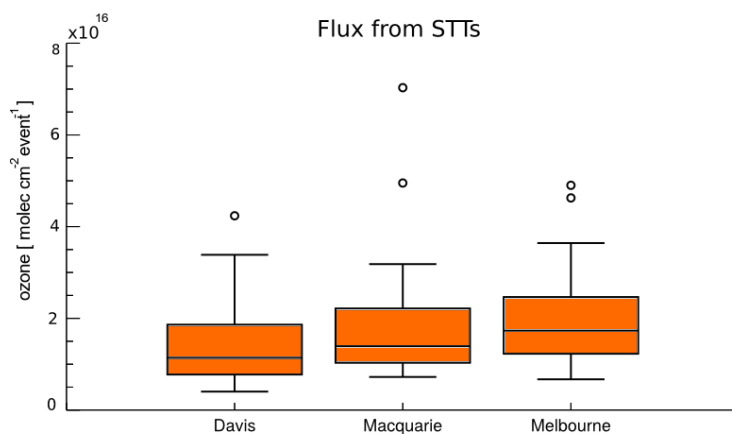

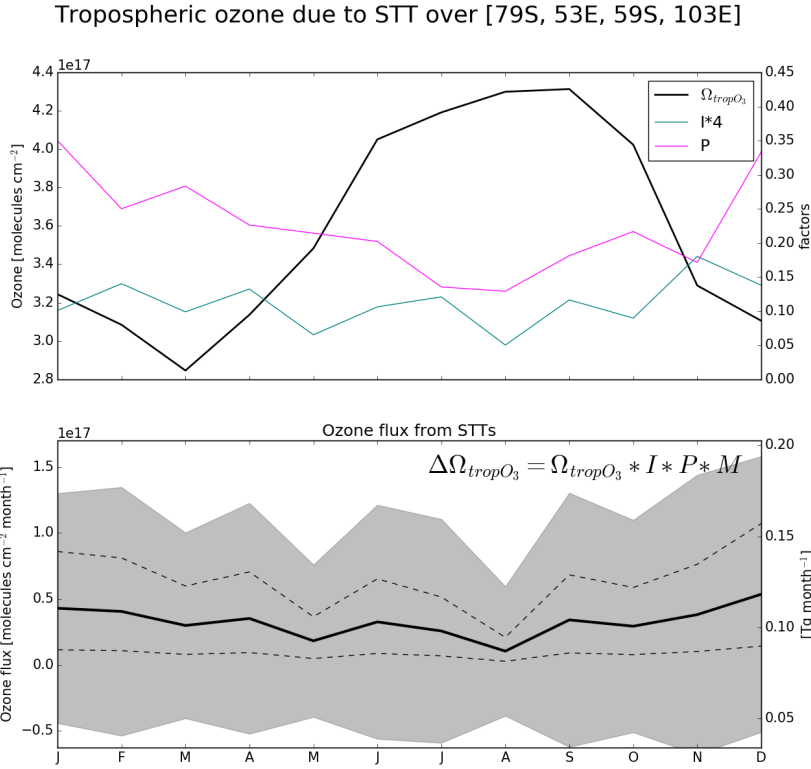**Figure 16.** Tropospheric ozone attributed to STT events, derived from ozonesonde measurements as described in the text.

Figure 17. (Top) The three quantities used to calculate the ozone flux from STT events over the region containing Macquarie Island and Melbourne. The tropospheric ozone column $\Omega_{Trop_{O_3}}$ (black, left axis) is from GEOS-Chem, while the STT probability P(magenta, right axis) and impact I (teal, right axis) are from the ozonesonde measurements. The STT impact is multiplied by 4 to better show the seasonality. (Bottom) Estimated contribution of STT to tropospheric ozone columns over the region, with range determined by the uncertainty estimated as outlined in Sect. 5.3. The black line shows STT ozone flux if event lifetime is assumed to be 2 days, with dashed lines showing flux if event lifetime was assumed to be either 1 day or 1 week.

of STT is calculated from fraction of ozonesonde releases for which an STT event was detected, within each month. If we assume events last N days, we find how many events per month by multiplying the days in a month by P and dividing by the assumed event lifetime. For example if we expect to see an event 25% of the time in a month, and events last one day, we expect one event every four days (~ 7.5 events in that month) whereas if we expect events to last a week then we would expect $\sim$one event in that month. This leads us to multiply our flux$_i$ by P, and then by the term M (M = days per month $/N$) determined by our assumed event lifetime in order to determine monthly STT ozone flux.

The upper panels in figures 17-19 show the factors I, P, and Ω_{O_3} which are used along with the assumed event lifetime to estimate the STT flux. The tropospheric ozone and area of our region is calculated using the output and surface area from
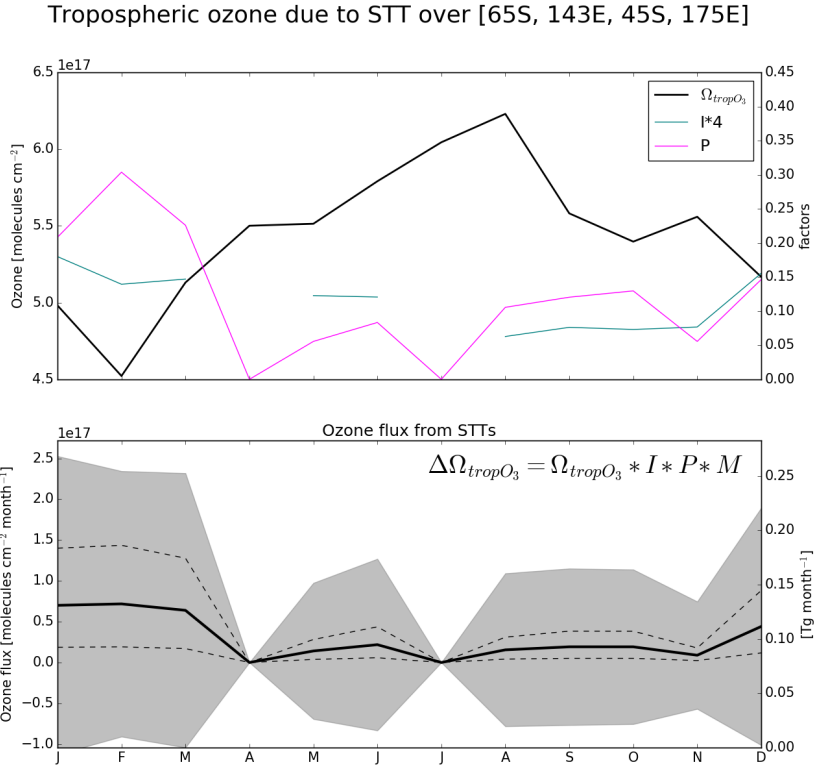
Figure 18. As described in 17, for the region containing Melbourne.

Table 3. Seasonal STT ozone contribution in the regions near each site, in kg km^{-2} month^{-1}.

Region	DJF	MAM	JJA	SON
Davis	10(382%)	13(325%)	11(405%)	13(353%)
Macqaurie	20(412%)	9(666%)	5(958%)	4(1267%)
Melbourne	195(223%)	18(500%)	5(1320%)	15(635%)

GEOS-Chem over the Southern Ocean grid boxes. The longevity of ozone events is very difficult to determine, and we've chosen 2 days as a representative number based on several examples in Lin et al. (2012) where intrusions were seen to last from 1-3 days (occasionally longer) and an analysis of one large event by Cooper et al. (2004) showing that most of the ozone had dispersed after 48 hours. The lower panel of these two figures show the results of the calculation when we choose 2 days for our flux estimation, with dotted lines showing the values calculated if we assume events last 1 day (upper bound of estimated flux) or one week (lower bound of estimated flux). Relative uncertainty in this M term is set to 50%, by setting the standard deviation equal to half of the magnitude of the term.
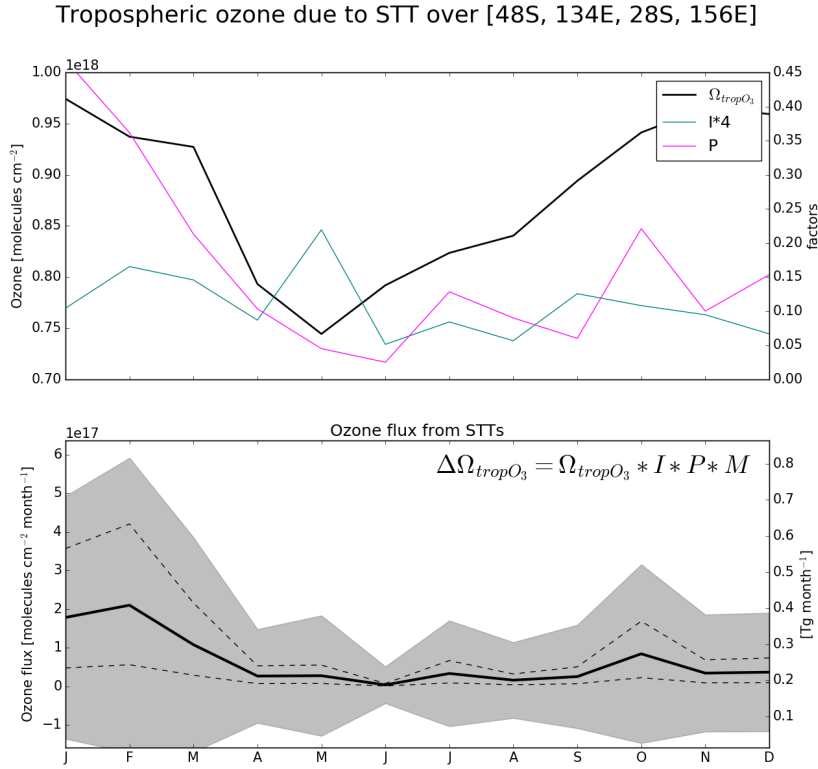
15

Figure 19. As described in 17, for the region containing Melbourne.

5.2 Results and comparisons

5 Škerlak et al. (2014) show an estimate of roughly 40 to 150 kg km^{-2} month^{-1} in these regions, over all seasons (see Fig. 16, 17 in their publication) while we estimate 4 to 20 kg km^{-2} month^{-1} STT impact, except for Summer (DJF) over Melbourne, which shows a large spike to 195 kg km^{-2} month^{-1}. Our calculated seasonal contributions, along with total uncertainty are shown in Table 3.

Two other previous studies have found STT ozone fluxes in the SH extratropics are largest from autumn or winter to early spring. **?** used PV and winds from the GEOS reanalysis combined with ozone measurements from the TOMS satellite to

5 estimate that the ozone flux between 30° S and 60° S 210 Tg yr^{-1}. **?** model the upper tropospheric ozone and it's source (emissions/lightning/stratospheric) over the Atlantic ocean between 30° S and 45° S, and suggest that most of this is transported from the stratosphere from March to September, which is when the subtropical jet system is strongest. The extrapolation over the entire southern ocean has been performed by extending the above calculations, however assuming such a large area is

homogeneous is not feasible. The results extrapolated over the southern ocean can be viewed in the supplementary section

10 (TODO: hardcode reference heresup:sec:SOExtrapolation).

5.3 Uncertainties

The uncertainties in our two regions of extrapolated ozone are determined from the standard deviations in monthly values over the multi-year dataset range. For each term; I, P, and Ω_{O_3}, the monthly averaged quantities are stored for each year where we have data, and then the standard deviation over the 7-10 values for each month are used to calculate the proportional uncertainty

5 for each parameter. In the case where only one event is recorded for a particular month (eg. June over Melbourne), uncertainty in I (the impact, which for this case has only one value) is set to 100%, and finally the proportional uncertainties are added to get the total flux estimate uncertainty. This ignores uncertainty due to the non-homogeneity of the regions extrapolated over, and would require more data, parameters, and analysis to apply to larger regions. The overall uncertainty as a percentage is shown in parentheses in Table 3, these values are on the order of 200%, largely due to uncertainty in the P and I factors which

10 both sit near 100% uncertainty for each month. The uncertainty in the I factor of our STT flux calculation is estimated from the standard deviation of the calculated values, for each of the three sites, as the variability in this term appears to be homoskedastic (unvarying in time). The P factor is assumed to follow a Bernoulli distribution, with variance calculated for each month at each site. Uncertainty in tropospheric ozone from GEOS-Chem is estimated using the standard deviation at each site, this term is also seen to be homoskedastic. Uncertainty in assumed event lifetime is set at 50%. These uncertainties propogate

15 to the STT flux calculation through the standard variance of a product of independent variables calculation: $var(\Pi_i X_i) = \Pi_i(var(X_i) + E(X_i)^2) - (\Pi_i E(X_i))^2$

Considering the I factor, as discussed in here and in Sect. 6, there are several uncertainties in our method that are likely to lead to a low bias, including a conservative estimate of flux within each event and a process that excludes potential events which are too close to the tropopause or to transported smoke plumes.

20 It is worth noting that this extrapolation is simplistic and is performed as an example of how the STT detection algorithm could be used. A more spatially resolved estimate could be determined by dividing the Southern Ocean region into longitudinal and latitudinal bins for calculating the average $\Omega_{SO_{O_3}}$ from GEOS-Chem, applying latitudinal gradients to P and I based on their values at the three sonde release sites, and adding longitudinal variability due to seasonal stratospheric wind jet streams (**??**). An improved estimate of event lifetime and parameterisation of how many events may be occuring simultaneously could

25 also be addressed, however this is beyond the scope of this work and in any case would not address all the limitations of the estimate provided herein.

Our estimate of the fraction of tropospheric ozone from each STT event (I) is likely to be biased low, perhaps by a significant amount. Using a global CTM with a stratospheric ozone tracer, **?** estimated that up to 30–40% of the ozone was transported from the stratosphere, for the ozone mixing ratio at 500 hPa in the northern hemisphere.

6 Sensitivities and limitations

Our method uses several subjectively defined quantities in the process of STT event detection. Here we briefly discuss these quantities and the sensitivity of the method to each. Using the algorithm discussed in Sect. 2.3, we detect 46 events at Davis, 47 (+8 fire influenced) events at Macquarie Island, and 73 (+14 fire influenced) events at Melbourne.

The cut-off threshold (defined separately for each site) is determined from the 99th percentile of the ozone perturbation profiles between 2 km above the earth's surface and 1 km below the tropopause. We use the 99th percentile because at this point the filter locates clear events with no obvious false positives. Event detection is highly sensitive to this choice; for example, using the 98.5th percentile instead increased detected events by 10 (22%) at Davis, 19 (40%) at Macquarie Island, and 24 (33%) at Melbourne. Event detection is therefore also sensitive to the range over which the percentile is calculated (2 km above the earth's surface to 1 km below the tropopause). This range was chosen to remove anomalous edge effects of the Fourier bandpass filter and to discount the highly variable ozone concentration which occurs near the tropopause.

Ozone enhancements are only considered STT events if they occur above 4 km and below 500 m below the tropopause. This range removes possible ground pollution and events not sufficiently separated from the stratosphere, while still capturing many well-defined events that occur within 1 km of the tropopause. An example of a well-defined event that occurs within 1 km of the tropopause is examined below in Fig. 6.

The event detection was less sensitive to the choice of Fourier bandpass scales: widening the allowed scales from the range 0.5-5.0 km to 0.4-5.1 km increased the detected events by 3 at Melbourne and 2 at Macquarie Island. Meanwhile, 2 fewer events were detected at Davis because the change to bandpass scales resulted in an increase in the threshold value calculated from the perturbed profiles (removing some detected events which were no longer larger than the new 99th percentile).

Overall, the method used here to detect STTs is conservative, and more events could be classified by changing some the parameters in the detection algorithm; however, this would increase the chance of misdiagnosis. For instance; when relaxing the ozone perturbation threshold to 98% several events are detected at each site which were not clear events (determined visually).

Uncertainties in STT ozone flux detection are also quite large ($\sim 200\%$), and could be directly improved with larger or longer datasets. Possible parameterisations and an improved model of event lifetime could also improve the confidence in our estimate of event impacts, as well as potentially removing some of our assumptions. The simple assumptions made in order to achieve an estimate of ozone flux are not feasible over larger areas, however as a preliminary or constraining estimate for a region with few measurements we believe they add to the discussion.

7 Conclusions

Stratosphere-to-troposphere transport (STT) can be a major source of ozone to the remote free troposphere, but the occurrence and influence of STT events remains poorly quantified in the southern hemisphere (SH) extratropics. Ozonesonde observations in the SH provide a satellite-independent quantification of the frequency of STT events, as well as an estimate of their impact and source. Using almost ten years of ozonesonde profiles over the southern high latitudes, we have quantified the frequency,

seasonality, and altitude distributions of STT events in the SH extratropics. By combining this information with ozone column estimates from a global chemical transport model, we provided a first, conservative estimate of the influence of STT events on tropospheric ozone over the Southern Ocean.

Our method involved applying a Fourier bandpass filter to the measured ozone profiles to determine STT event occurrence and strength. The filter removed seasonal influences and allowed clear detection of ozone-enhanced tongues of air in the troposphere. By setting empirically-derived thresshholds, this method clearly distinguished tropospheric ozone enhancements that are separated from the stratosphere. Our method is sensitive to various parameters involved in the calculation; however, for our sites we saw no false positive detections of STT events.

Detected STT events at three sites spanning the SH extra-tropics (38°S, 55°S, and 69°S) showed a distinct seasonal cycle. All three sites displayed a summer (DJF) maximum and winter (JJA) minimum, although the seasonal amplitude was less apparent at the Antarctic site (Davis) as events were also detected regularly in winter and spring (likely due to polar jet stream-caused turbulence). Comparison with ERA-Interim reanalysis data suggested the majority of events were caused by turbulent weather in the upper troposphere due to low pressure fronts, followed by cut-off low pressure systems. Comparison of ozonesonde-measured ozone profiles against those simulated by the GEOS-Chem global chemical transport model showed the model is able to reproduce seasonal features but does not have sufficient vertical resolution to distinguish STT events.

By combining the simulated tropospheric column ozone from GEOS-Chem with ozonesonde-derived STT estimates, we provide a first estimate of the total contribution of STT events to tropospheric ozone over the Southern Ocean. We conservatively estimated that the ozone enhancement due to STT events at our three sites ranges from TODO: range of local to site calculations.

Estimating STT flux using ozonesonde data alone remains challenging; however, the very high vertical resolution provided by ozonesondes means they are capable of detecting STT events that models, reanalyses, and satellites may not. Further work is needed to more accurately translate these ozonesonde measurements into STT ozone fluxes, particularly in the SH where data are sparse and STT is likely to be a major contributor to upper tropsopheric ozone in some regions. More frequent ozonesonde releases at SH sites would facilitate development of better STT flux estimates for this region.

References

Cooper, O., Forster, C., Parrish, D., Dunlea, E., Hübler, G., Fehsenfeld, F., Holloway, J., Oltmans, S., Johnson, B., Wimmers, A., and Horowitz, L.: On the life cycle of a stratospheric intrusion and its dispersion into polluted warm conveyor belts, Journal of Geophysical Research D: Atmospheres, 109, 1–18, doi:10.1029/2003JD004006, 2004.

Jacobson, M. C. and Hansson, H.: Organic atmospheric aerosols: Review and state of the science, Reviews of Geophysics, pp. 267–294, doi:10.1029/1998RG000045, 2000.

Jaffe, D. a. and Wigder, N. L.: Ozone production from wildfires: A critical review, Atmospheric Environment, 51, 1–10, doi:10.1016/j.atmosenv.2011.11.063, http://dx.doi.org/10.1016/j.atmosenv.2011.11.063, 2012.

Langford, A. O., Brioude, J., Cooper, O. R., Senff, C. J., Alvarez, R. J., Hardesty, R. M., Johnson, B. J., and Oltmans, S. J.: Stratospheric influence on surface ozone in the Los Angeles area during late spring and early summer of 2010, Journal of Geophysical Research Atmospheres, 117, 1–17, doi:10.1029/2011JD016766, 2012.

Lin, M., Fiore, A. M., Cooper, O. R., Horowitz, L. W., Langford, A. O., Levy, H., Johnson, B. J., Naik, V., Oltmans, S. J., and Senff, C. J.: Springtime high surface ozone events over the western United States: Quantifying the role of stratospheric intrusions, Journal of Geophysical Research Atmospheres, 117, 1–20, doi:10.1029/2012JD018151, 2012.

Lin, M., Fiore, A. M., Horowitz, L. W., Langford, A. O., Oltmans, S. J., Tarasick, D., and Rieder, H. E.: Climate variability modulates western US ozone air quality in spring via deep stratospheric intrusions., Nature communications, 6, 7105, doi:10.1038/ncomms8105, http://www.nature.com/ncomms/2015/150512/ncomms8105/full/ncomms8105.html, 2015.

Monks, P. S., Archibald, A. T., Colette, A., Cooper, O., Coyle, M., Derwent, R., Fowler, D., Granier, C., Law, K. S., Mills, G. E., Stevenson, D. S., Tarasova, O., Thouret, V., von Schneidemesser, E., Sommariva, R., Wild, O., and Williams, M. L.: Tropospheric ozone and its precursors from the urban to the global scale from air quality to short-lived climate forcer, Atmospheric Chemistry and Physics, 15, 8889–8973, doi:10.5194/acp-15-8889-2015, http://www.atmos-chem-phys.net/15/8889/2015/, 2015.

Pak, B., Langenfelds, R., Young, S., Francey, R., Meyer, C., Kivlighon, L., Cooper, L., Dunse, B., Allison, C., Steele, L., Galbally, I., and Weeks, I.: Measurements of biomass burning influences in the troposphere over southeast Australia during the SAFARI 2000 dry season campaign, Journal of Geophysical Research D: Atmospheres, 108, 1–10, doi:10.1029/2002JD002343, http://www.scopus.com/inward/record.url?eid=2-s2.0-0742322536&partnerID=40&md5=cafaeef03b948fb456696583ed3ab9a5, 2003.

Reutter, P., Škerlak, B., Sprenger, M., and Wernli, H.: Stratosphere-troposphere exchange (STE) in the vicinity of North Atlantic cyclones, Atmospheric Chemistry and Physics, 15, 10 939–10 953, doi:10.5194/acp-15-10939-2015, 2015.

Škerlak, B., Sprenger, M., and Wernli, H.: A global climatology of stratosphere-troposphere exchange using the ERA-Interim data set from 1979 to 2011, Atmospheric Chemistry and Physics, 14, 913–937, doi:10.5194/acp-14-913-2014, http://www.atmos-chem-phys.net/14/913/2014/, 2014.

Stevenson, D. S., Young, P. J., Naik, V., Lamarque, J. F., Shindell, D. T., Voulgarakis, a., Skeie, R. B., Dalsoren, S. B., Myhre, G., Berntsen, T. K., Folberth, G. a., Rumbold, S. T., Collins, W. J., MacKenzie, I. a., Doherty, R. M., Zeng, G., Van Noije, T. P. C., Strunk, a., Bergmann, D., Cameron-Smith, P., Plummer, D. a., Strode, S. a., Horowitz, L., Lee, Y. H., Szopa, S., Sudo, K., Nagashima, T., Josse, B., Cionni, I., Righi, M., Eyring, V., Conley, a., Bowman, K. W., Wild, O., and Archibald, a.: Tropospheric ozone changes, radiative forcing and attribution to emissions in the Atmospheric Chemistry and Climate Model Intercomparison Project (ACCMIP), Atmospheric Chemistry and Physics, 13, 3063–3085, doi:10.5194/acp-13-3063-2013, 2013.

Thompson, A. M., Balashov, N. V., Witte, J. C., Coetzee, J. G. R., Thouret, V., and Posny, F.: Tropospheric ozone increases over the southern Africa region: Bellwether for rapid growth in Southern Hemisphere pollution?, Atmospheric Chemistry and Physics, 14, 9855–9869, doi:10.5194/acp-14-9855-2014, 2014.

Wauben, W. M. F., Fortuin, J. P. F., and Velthoven, P. F. J. V.: Comparison of modeled ozone distributions observations, Journal of Geophysical
35   Research, 103, 3511–3530, 1998.

Young, P. J., Naik, V., Voulgarakis, A., Fiore, A. M., Horowitz, L. W., Lamarque, J. F., Lin, M., Prather, M. J., Bergmann, D., Cameron-Smith, P. J., Cionni, I., Collins, W. J., Dalsøren, S. B., Doherty, R., Eyring, V., Faluvegi, G., Folberth, G. A., Josse, B., Lee, Y. H., MacKenzie, I. A., Nagashima, T., Van Noije, T. P. C., Plummer, D. A., Righi, M., Rumbold, S. T., Skeie, R., Shindell, D. T., Stevenson, D. S., Strode, S., Sudo, K., Szopa, S., and Zeng, G.: Preindustrial to present-day changes in tropospheric hydroxyl radical and methane lifetime from the Atmospheric Chemistry and Climate Model Intercomparison Project (ACCMIP), Atmospheric Chemistry and Physics, 13, 5277–5298,
5   doi:10.5194/acp-13-5277-2013, 2013.

Zanis, P., Hadjinicolaou, P., Pozzer, A., Tyrlis, E., Dafka, S., Mihalopoulos, N., and Lelieveld, J.: Summertime free-tropospheric ozone pool over the eastern Mediterranean/middle east, Atmospheric Chemistry and Physics, 14, 115–132, doi:10.5194/acp-14-115-2014, 2014.